

Designs for optical cloaking with high-order transformations

Wenshan Cai, Uday K. Chettiar, Alexander V. Kildishev, and Vladimir M. Shalaev*

*School of Electrical and Computer Engineering and Birck Nanotechnology Center, Purdue University,
West Lafayette, Indiana 47907, USA*

*Corresponding author: shalaev@purdue.edu

Abstract: Recent advances in metamaterial research have provided us a blueprint for realistic cloaking capabilities, and it is crucial to develop practical designs to convert concepts into real-life devices. We present two structures for optical cloaking based on high-order transformations for TM and TE polarizations respectively. These designs are possible for visible and infrared wavelengths. This critical development builds upon our previous work on nonmagnetic cloak designs and high-order transformations.

©2008 Optical Society of America

OCIS codes: (230.3205) Invisibility cloaks; (160.3918) Metamaterials; (160.4760) Optical properties.

References and links

1. G. W. Milton, and N. A. P. Nicorovici, "On the cloaking effects associated with anomalous localized resonance," *Proc. R. Soc. London, Ser. A* **462**, 3027-3059 (2006).
2. N. A. P. Nicorovici, G. W. Milton, R. C. McPhedran, and L. C. Botten, "Quasistatic cloaking of two-dimensional polarizable discrete systems by anomalous resonance," *Opt. Express* **15**, 6314-6323 (2007).
3. A. Alu, and N. Engheta, "Achieving transparency with plasmonic and metamaterial coatings," *Phys. Rev. B* **72**, 016623 (2005).
4. M. G. Silveirinha, A. Alu, and N. Engheta, "Parallel-plate metamaterials for cloaking structures," *Phys. Rev. B* **75**, 036603 (2007).
5. D. A. B. Miller, "On perfect cloaking," *Opt. Express* **14**, 12457-12466 (2006).
6. F. J. Garcia de Abajo, G. Gomez-Santos, L. A. Blanco, A. G. Borisov, and S. V. Shabanov, "Tunneling mechanism of light transmission through metallic films," *Phys. Rev. Lett.* **95**, 067403 (2005).
7. A. Greenleaf, M. Lassas, and G. Uhlmann, "Anisotropic conductivities that cannot be detected by EIT," *Physiol. Meas.* **24**, 413-419 (2003).
8. Y. Benveniste, and T. Miloh, "Neutral inhomogeneities in conduction phenomena," *J. Mech. Phys. Solids* **47**, 1873-1892 (1999).
9. A. Hendi, J. Henn, and U. Leonhardt, "Ambiguities in the scattering tomography for central potentials," *Phys. Rev. Lett.* **97**, 073902 (2006).
10. J. B. Pendry, D. Schurig, and D. R. Smith, "Controlling electromagnetic fields," *Science* **312**, 1780-1782 (2006).
11. U. Leonhardt, "Optical conformal mapping," *Science* **312**, 1777-1780 (2006).
12. D. Schurig, J. B. Pendry, and D. R. Smith, "Calculation of material properties and ray tracing in transformation media," *Opt. Express* **14**, 9794-9804 (2006).
13. D. Schurig, J. J. Mock, B. J. Justice, S. A. Cummer, J. B. Pendry, A. F. Starr, and D. R. Smith, "Metamaterial electromagnetic cloak at microwave frequencies," *Science* **314**, 977-980 (2006).
14. W. Cai, U. K. Chettiar, A. V. Kildishev, and V. M. Shalaev, "Optical cloaking with metamaterials," *Nat. Photonics* **1**, 224-227 (2007).
15. W. Cai, U. K. Chettiar, A. V. Kildishev, V. M. Shalaev, and G. W. Milton, "Nonmagnetic cloak with minimized scattering," *Appl. Phys. Lett.* **91**, 111105 (2007).
16. R. Weder, "A rigorous analysis of high-order electromagnetic invisibility cloaks," *J. Phys. A: Math. Theor.* **41**, 065207 (2008).
17. D. E. Aspnes, "Optical-Properties of Thin-Films," *Thin Solid Films* **89**, 249-262 (1982).
18. S. A. Ramakrishna, J. B. Pendry, M. C. K. Wiltshire, and W. J. Stewart, "Imaging the near field," *J. Mod. Opt.* **50**, 1419-1430 (2003).
19. D. Schurig, and D. R. Smith, "Sub-diffraction imaging with compensating bilayers," *New J. Phys.* **7**, 162 (2005).

20. P. A. Belov, and Y. Hao, "Subwavelength imaging at optical frequencies using a transmission device formed by a periodic layered metal-dielectric structure operating in the canalization regime," *Phys. Rev. B* **73**, 113110 (2006).
21. S. M. Feng, and J. M. Elson, "Diffraction-suppressed high-resolution imaging through metalodielectric nanofilms," *Opt. Express* **14**, 216-221 (2006).
22. Z. Jacob, L. V. Alekseyev, and E. Narimanov, "Optical hyperlens: Far-field imaging beyond the diffraction limit," *Opt. Express* **14**, 8247-8256 (2006).
23. A. Salandrino, and N. Engheta, "Far-field subdiffraction optical microscopy using metamaterial crystals: Theory and simulations," *Phys. Rev. B* **74**, 075103 (2006).
24. O. Wiener, "Die Theorie des Mischkorpers für das Feld der stationären Stromung," *Abh. Math.-Phys. Klasse Königlich Sachsischen Des. Wiss.* **32**, 509-604 (1912).
25. D. E. Aspnes, "Bounds on Allowed Values of the Effective Dielectric Function of 2-Component Composites at Finite Frequencies," *Phys. Rev. B* **25**, 1358-1361 (1982).
26. D. J. Bergman, "Exactly Solvable Microscopic Geometries and Rigorous Bounds for the Complex Dielectric-Constant of a 2-Component Composite-Material," *Phys. Rev. Lett.* **44**, 1285-1287 (1980).
27. G. W. Milton, "Bounds on the Complex Dielectric-Constant of a Composite-Material," *Appl. Phys. Lett.* **37**, 300-302 (1980).
28. P. B. Johnson, and R. W. Christy, "Optical-Constants of Noble-Metals," *Phys. Rev. B* **6**, 4370-4379 (1972).
29. E. D. Palik, *Handbook of Optical Constants of Solids* (Academic Press, New York, 1997).
30. W. G. Spitzer, D. Kleinman, and D. Walsh, "Infrared Properties of Hexagonal Silicon Carbide," *Phys. Rev.* **113**, 127-132 (1959).
31. D. Korobkin, Y. Urzhumov, and G. Shvets, "Enhanced near-field resolution in midinfrared using metamaterials," *J. Opt. Soc. Am. B* **23**, 468-478 (2006).
32. T. Taubner, D. Korobkin, Y. Urzhumov, G. Shvets, and R. Hillenbrand, "Near-field microscopy through a SiC superlens," *Science* **313**, 1595-1595 (2006).
33. J. A. Schuller, R. Zia, T. Taubner, and M. L. Brongersma, "Dielectric metamaterials based on electric and magnetic resonances of silicon carbide particles," *Phys. Rev. Lett.* **99**, 107401 (2007).
34. S. O'Brien, and J. B. Pendry, "Photonic band-gap effects and magnetic activity in dielectric composites," *J. Phys. Condens. Matter.* **14**, 4035-4044 (2002).
35. K. C. Huang, M. L. Povinelli, and J. D. Joannopoulos, "Negative effective permeability in polaritonic photonic crystals," *Appl. Phys. Lett.* **85**, 543-545 (2004).
36. M. S. Wheeler, J. S. Aitchison, and M. Mojahedi, "Three-dimensional array of dielectric spheres with an isotropic negative permeability at infrared frequencies," *Phys. Rev. B* **72**, 193103 (2005).
37. L. Peng, L. X. Ran, H. S. Chen, H. F. Zhang, J. A. Kong, and T. M. Grzegorzcyk, "Experimental observation of left-handed behavior in an array of standard dielectric resonators," *Phys. Rev. Lett.* **98**, 157403 (2007).

1. Introduction

Cloaking (or being invisible) is a longtime dream that may date back to the very beginning of human civilization. In the last few years, this dream moves one step closer to reality, thanks to various schemes proposed to control and manipulate electromagnetic waves in unprecedented ways [1-6]. From among these methods, the transformation approach, which generalized a similar idea on cloaking of thermal conductivity [7, 8], has generated enormous interest [9-12], partially because of its similarity to the mythological version of cloak: a closed surface is created which renders arbitrary objects within its interior invisible to detection. The constitutive parameters of the cloak are determined by the specific form of the spatial transformation. They are usually anisotropic with gradient requirements that are only possible using artificially engineered structures, such as the previously demonstrated microwave cloak [13].

The word "invisible" naturally implies the inaccessibility of an object to waves with wavelengths perceivable by human eyes, which are so-called "visible light". Unfortunately, an electromagnetic cloak working at optical frequencies has yet to be demonstrated, although a conceptual design with reduced non-magnetic parameters has been discussed by the present authors [14]. Recently we also proposed non-magnetic cloaks based on high-order transformations [15], which may provide not only better cloaking performance, but also more flexibility in determining the properties of constitutive materials. A rigorous analysis of high-order cloaks was presented afterwards in [16]. As a critical development of our recent work

[14, 15], in this paper we propose two practical designs of optical cloaks based on high-order transformations. Specifically, we demonstrate i) a non-magnetic cylindrical cloaking system for TM incidence (magnetic field polarized along the cylindrical axis) which consists of a layered metal-dielectric without any variation in either material or structure along the vertical direction; ii) a magnetic cylindrical cloak for TE incidence (electric field polarized parallel to axis) utilizing Mie resonance in periodic rod-shaped high-permittivity materials. In each scheme, through careful design of the geometry, the anisotropy and gradient of material properties in the cloaking shell fits remarkably well to the intended transformation.

2. Material properties in cylindrical cloaks

For a cloak in the cylindrical geometry, a coordinate transformation function $r = g(r')$ from (r', θ', z') to (r, θ, z) is used to compress the region $r' \leq b$ into a concentric shell of $a \leq r \leq b$, and the permittivity and permeability tensors required for an exact cloak can be determined as [15]:

$$\varepsilon_r = \mu_r = \left(r'/r\right) \partial g(r') / \partial r'; \quad \varepsilon_\theta = \mu_\theta = 1/\varepsilon_r; \quad \varepsilon_z = \mu_z = \left(r'/r\right) \left[\partial g(r') / \partial r'\right]^{-1} \quad (1)$$

For the standard states of incident polarization, the requirement in Eq. (1) can be relaxed such that only three of the six components are relevant. For example, for TE (TM) polarization, only ε_z , μ_r and μ_θ (μ_z , ε_r and ε_θ) enter into Maxwell's equations. Moreover, the parameters can be further simplified to form reduced parameters which are more realistic for practical applications. Since the trajectory of the waves is determined by the cross product components of the ε and μ tensors instead of the two tensors individually, the cloaking performance is sustained as long as $n_\theta = \sqrt{\varepsilon_z \mu_r}$ and $n_r = \sqrt{\varepsilon_z \mu_\theta}$ ($n_\theta = \sqrt{\mu_z \varepsilon_r}$ and $n_r = \sqrt{\mu_z \varepsilon_\theta}$) are kept the same as those determined by values in Eq. (1). This technique results in a specific set of reduced parameters which allow for a permeability gradient along only the radial direction for the TE mode [13]:

$$\mu_r = \left(r'/r\right)^2 \left[\partial g(r') / \partial r'\right]^2; \quad \mu_\theta = 1; \quad \varepsilon_z = \left[\partial g(r') / \partial r'\right]^{-2} \quad (2)$$

and can be purely non-magnetic for the TM mode [14]:

$$\varepsilon_r = \left(r'/r\right)^2; \quad \varepsilon_\theta = \left[\partial g(r') / \partial r'\right]^{-2}; \quad \mu_z = 1 \quad (3)$$

From an application point of view, the design of an electromagnetic cloak is meant to elaborate realistic structures and materials which fulfill the set of parameters corresponding to any of Eqs. (1-3). The reported experimental demonstration of a microwave cloak in [13] presented a structure where Eq. (2) was satisfied, and the proposed non-magnetic optical cloak in [14] corresponded to the case described by Eq. (3). One common feature shared in the two systems is that both works obtained designs based on a standard linear transformation $r = g(r') = (1 - a/b)r' + a$. In sharp contrast to the previous work, the purpose of this paper is to present realistic designs based on more general high-order transformations. In particular, for the TM polarization, we propose a non-magnetic cloak design compatible with mature fabrication techniques such as direct deposition and direct etching; for TE incidence, we present a structure that allows for a radial gradient in the magnetic permeability while avoiding the use of plasmonic metallic units in the optical range.

3. Optical cloak with high-order transformations I: TM mode

First we focus on the non-magnetic cloak in the TM mode with parameters given in Eq. (3). In this case, the design of cloak is essentially to produce the required gradient in ε_r and ε_θ using readily available materials. Apparently, a cloak cannot consist of only a single-constituent material, because a spatial variation in material properties is critical to building a cloak. To start the design, we first examine the overall flexibility we can achieve in the effective permittivity of a general two-phase composite medium. When an external field interacts with

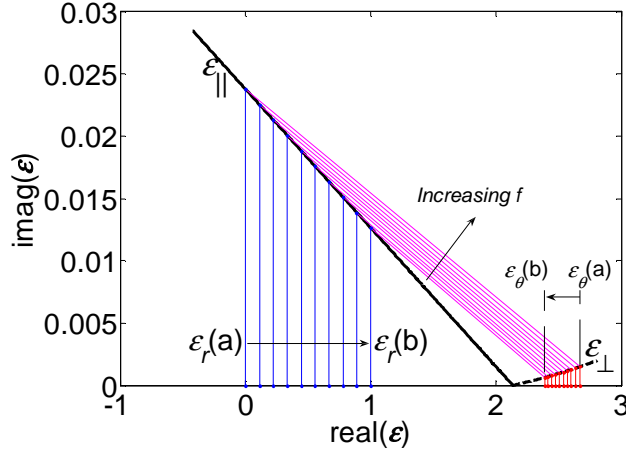


Fig. 1. The principle of constructing a non-magnetic cloak in the TM mode with high-order transformations. The thick solid and dashed lines represent the two Wiener bounds $\varepsilon_{\parallel}(f)$ and $\varepsilon_{\perp}(f)$, respectively. Basic material properties for this calculation: $\varepsilon_1 = \varepsilon_{Ag} = -10.6 + 0.14i$ and $\varepsilon_2 = \varepsilon_{SiO_2} = 2.13$ at $\lambda = 532$ nm.

a composite consisting of two elements with permittivity of ε_1 and ε_2 respectively, minimal screening occurs when all internal boundaries between the two constituents are parallel to the electric field, and maximal screening happens when all boundaries aligned perpendicular to the field. These two extremes are possible in an alternating layered structure, provided that the thickness of each layer is much less than the wavelength of incidence [17]. In this case the two extreme values of the effective permittivity can be approximated as

$$\varepsilon_{\parallel} = f\varepsilon_1 + (1-f)\varepsilon_2; \quad \varepsilon_{\perp} = \varepsilon_1\varepsilon_2 / (f\varepsilon_2 + (1-f)\varepsilon_1) \quad (4)$$

where f and $1-f$ denote the volume fractions of components 1 and 2, and the subscripts \parallel and \perp indicate the cases with electric field polarized parallel and perpendicular to the interfaces of the layers, respectively. Such layered structures have been studied extensively in recent years for various purposes, especially in sub-diffraction imaging for both the near field and the far zone [18-23].

The two extrema in Eq. (4) are called the Wiener bounds to permittivity, which set the absolute bound on all possible values of the effective permittivity of a two-phase composite [24, 25]. In realistic composites, more strict limits, for example those from the spectral representation developed by Bergman and Milton [26, 27], might apply in addition to the Wiener bounds, but Eq. (4) nonetheless provides a straightforward way to evaluate the accessible permittivity in a composite with given constituent materials. The Wiener bounds can be illustrated on a complex ε -plane with the real and imaginary parts of ε being the x and y axis, respectively. In this plane, the low-screening bound in Eq. (4a) corresponds to a straight line between ε_1 and ε_2 , and the high-screening bound in Eq. (4b) defines an arc which is part of the circle determined by the three points ε_1 , ε_2 and the origin.

The required material properties for the cloak in Eq. (3) indicates that, for a non-magnetic cylindrical cloak with any transformation function, ε_r varies from 0 at the inner boundary of the cloak ($r = a$) to 1 at the outer surface ($r = b$), while ε_{θ} is a function of r with varying positive value, except for the linear transformation case where $\partial g(r') / \partial r'$ is a constant. Now

we can evaluate the possibility of fulfilling the required parameters in Eq. (3) based on alternating metal-dielectric slices whose properties are estimated by Eq. (4). With phase 1 being a metal ($\varepsilon_1 = \varepsilon_m < 0$) and phase 2 representing a dielectric ($\varepsilon_2 = \varepsilon_d > 0$), the desired material properties of the cloak are only possible when the slices are within the r - z plane of the cylindrical coordinates. In this case ε_r and ε_{θ} correspond to ε_{\parallel} and ε_{\perp} in Eq. (4), respectively. This scenario is illustrated in Fig. 1. The thick solid and dashed lines represent

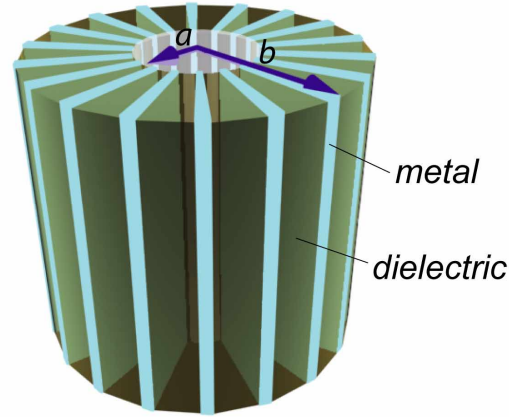


Fig. 2. Schematic of a cylindrical non-magnetic cloak with high-order transformations for TM polarization.

the two Wiener bounds $\epsilon_{\parallel}(f)$ and $\epsilon_{\perp}(f)$ respectively. The constituent materials used for the calculation are silver and silica at a green light wavelength of 532 nm. The pair of points on the bounds with the same filling fraction are connected with a straight line for clarification purposes. When ϵ_r changes between 0 and 1, the value of ϵ_{θ} varies accordingly as shown by the arrow between the two thin dashed lines. Therefore, the construction of a non-magnetic cloak requires that the relationship between the two quantities ϵ_{\parallel} and ϵ_{\perp} (as functions of f) within the range shown in Fig. 1 fits the material properties given in Eq. (3) for a particular transformation function $r = g(r')$. Another attractive feature of the proposed scheme is the minimal loss factor. As shown in Fig. 1, the loss feature described by the imaginary part of the effective permittivity is on the order of 0.01, much smaller than that of a pure metal or any resonant metal-dielectric structures. A schematic of the proposed structure consisting of interlaced metal and dielectric slices is illustrated in Fig. 2.

Mathematically, for a preset operational wavelength we seek a transformation together with the cylindrical shape factor a/b that fulfills the following equation:

$$\epsilon_m \epsilon_d \left(\frac{\partial g(r')}{\partial r'} \right)^2 + \left(\frac{r'}{g(r')} \right)^2 - (\epsilon_m + \epsilon_d) = 0 \quad (5)$$

and

$$g(0) = a; \quad g(b) = b; \quad \partial g(r') / \partial r' > 0 \quad (6)$$

There does not exist an exact analytical solution to the equations above. However, we may use polynomial functions to approach a possible solution. More specifically, a quadratic function in the following form

$$r = g(r') = \left[1 - a/b + p(r' - b) \right] r' + a \quad (7)$$

with $|p| < (b - a)/b^2$ can serve as a good candidate for an approximate solution to Eq. (5).

Table 1. Approximate quadratic transformations and materials for constructing a cloak with alternating slices

λ	ϵ_1	ϵ_2	$p \times (b^2/a)$	a/b
488 nm	$\epsilon_{Ag} = -8.15 + 0.11i$	$\epsilon_{SiO_2} = 2.14$	0.0662	0.389
532 nm	$\epsilon_{Ag} = -10.6 + 0.14i$	$\epsilon_{SiO_2} = 2.13$	0.0517	0.370
589.3 nm	$\epsilon_{Ag} = -14.2 + 0.19i$	$\epsilon_{SiO_2} = 2.13$	0.0397	0.354
632.8 nm	$\epsilon_{Ag} = -17.1 + 0.24i$	$\epsilon_{SiO_2} = 2.12$	0.0333	0.347
11.3 μ m	$\epsilon_{SiC} = -7.1 + 0.40i$	$\epsilon_{BaF_2} = 1.93$	0.0869	0.356

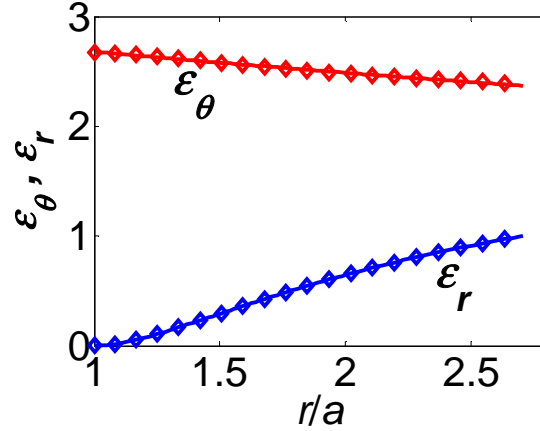


Fig. 3. Anisotropic material parameters ε_r and ε_θ of a non-magnetic cloak made of silver-silica alternating slices corresponding to the third row ($\lambda = 532$ nm) in Table 1. The solid lines represent the exact parameters determined by Eq. (2), and the diamond markers show the parameters on the Wiener's bounds given by Eq. (4).

Such a transformation automatically satisfies the boundary and monotonicity requirements in Eq. (6), and it is possible to fulfill Eq. (5) with minimal deviation when a proper shape factor is chosen. In Table 1 we provide transformations, materials and geometries for non-magnetic cloaks designed for several important frequency lines across the visible range including 488 nm (Ar-ion laser), 532 nm (Nd:YAG laser), 589.3 nm (sodium D-line), and 632.8 nm (He-Ne laser). In the calculations, the permittivity of silver is taken from well accepted experimental data [28], and the dielectric constant of silica is from the tabulated data in [29]. Note that the same design and transformation work for all similar cylindrical cloaks with the same shape factor a/b . When the approximate quadratic function is fixed for a given wavelength, the filling fraction function $f(r)$ is determined by the following equation:

$$f(r) = \frac{\text{Re}(\varepsilon_d) - \left(g^{-1}(r)/r\right)^2}{\text{Re}(\varepsilon_d - \varepsilon_m)} \quad (8)$$

As an example, in Fig. 3 we show the anisotropic material properties of a non-magnetic cloak corresponding to the $\lambda = 532$ nm case in Table 1. Our calculation shows that with the approximate quadratic transformation, the effective parameters ε_r and ε_θ obtained with the Wiener bounds in Eq. (4) fit with the exact parameters required for this transformation by Eq. (2) remarkably well, with the average deviation of less than 0.5%.

Compared to the previously designed cloak in [14] which requires thin metal needles embedded in a dielectric host following a pre-designed distribution, the fabrication feasibility of the newly proposed design is obvious because such vertical wall-like structures are compatible with mature fabrication techniques like direct deposition and direct etching.

4. Optical cloak with high-order transformations II: TE mode

In the next part of the paper, we focus on constructing a cylindrical cloak for TE mode working within the mid-infrared frequency range with a gradient in the magnetic permeability, as requested by Eq. (2). An electromagnetic cloak operating at mid-infrared is of great military and civilian interests, because this wavelength range corresponds to the thermal radiation band from human bodies. For this purpose there could be several different approaches which all involve silicon carbide, an important media for metamaterial research in mid-infrared. SiC is a polaritonic material with its phonon resonance band falling into the spectral range centered at around $12.5 \mu\text{m}$ (800 cm^{-1}), which introduces a sharp Lorentz behavior in its electric permittivity. The dielectric function of SiC at mid-infrared is well described with the following model [30, 31]:

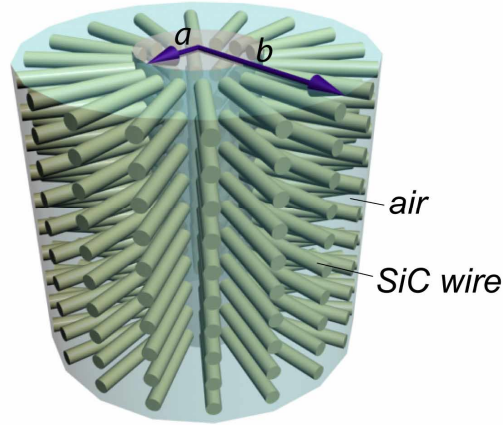


Fig. 4. Schematic of a cylindrical non-magnetic cloak with high-order transformations for TE polarization.

$$\varepsilon_{SiC} = \varepsilon_{\infty} \left[\frac{\omega^2 - \omega_L^2 + i\gamma\omega}{\omega^2 - \omega_T^2 + i\gamma\omega} \right] \quad (9)$$

where $\varepsilon_{\infty} = 6.5$, $\omega_L = 972 \text{ cm}^{-1}$, $\omega_T = 796 \text{ cm}^{-1}$ and $\gamma = 5 \text{ cm}^{-1}$. On the high-frequency side, the dielectric function is strongly negative, which makes its optical response similar to that of metals and has been utilized in applications like a mid-infrared superlens [31, 32]. At frequencies lower than the resonance frequency, the permittivity can be strongly positive, which makes SiC an attractive candidate for producing high-permittivity Mie resonators at the mid-infrared wavelength range [33].

SiC structures can be used to build mid-infrared cloaking devices in different styles. For example, we may consider using the needle-based structure detailed in [14] for the TM mode, where needles made of a low-loss negative- ε polaritonic material like SiC or TiO_2 are embedded in an IR transparent dielectric like ZnS. The non-magnetic cloak using alternating slices structure as proposed in this paper provides a more realistic design. With SiC as the negative- ε material and BaF_2 as the positive- ε slices with material properties given in [29], we can find the appropriate transformation function and shape factor that fulfills the material property requirements at a preset wavelength. The result for $\lambda = 11.3 \text{ }\mu\text{m}$ (CO_2 laser range) is shown in the last row of Table 1.

Now we consider a cylindrical cloak for the TE mode with the required material properties given in Eq. (2), which indicates that a gradient in the magnetic permeability along the radial direction is necessary. To be more specific, μ_r varies from 0 at the inner boundary ($r = a$) to $\left[\frac{\partial g(r')}{\partial r'} \right]^2$ at the outer surface ($r = b$), while the required ε_z changes accordingly following the function $\left[\frac{\partial g(r')}{\partial r'} \right]^{-2}$. The magnetic requirement may be accomplished using metal elements like split-ring resonators, coupled nanostrips or nanowires. However, such plasmonic structures inevitably exhibit a high loss, which is detrimental to the cloaking performance. A SiC based structure provides an all-dielectric route to a magnetic cloak for the TE mode due to the Mie resonance in a subwavelength SiC unit.

Meta-magnetic responses and a negative index of refraction in structures made from high-permittivity materials have been studied extensively in recently years [33-37]. Magnetic resonance in a rod-shaped high-permittivity particle can be excited by different polarizations of the external field with respect to the rod axis. When a strong magnetic resonance and an effective permeability substantially distinct from 1 are desired, the rod should be aligned parallel to the electric field to assure the maximum possible interaction between the rod and the external field. In our conceptual design of a cylindrical cloak for the TE mode, the desired

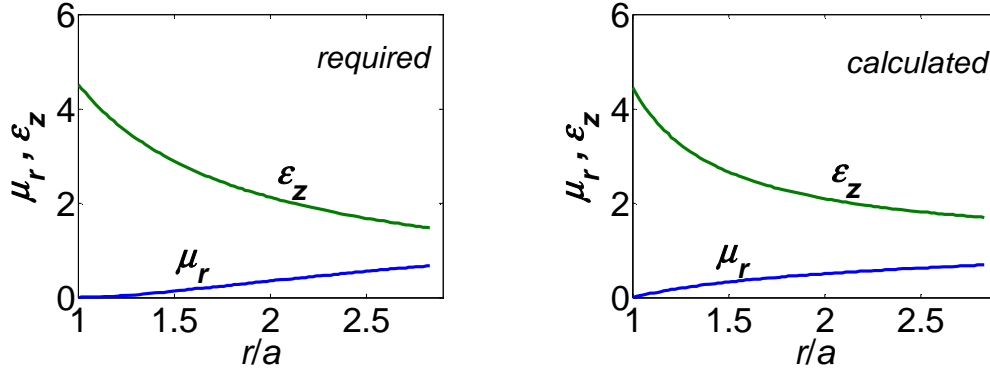


Fig. 5. The required and the calculated effective parameters μ_r and ϵ_z for a cylindrical TE cloak with SiC wire arrays for $\lambda = 13.5 \mu\text{m}$.

radial permeability has values of less than (but close to) 1, and resonance behavior in the effective permittivity ϵ_z should be avoided for a minimal loss. Therefore, with the electrical field polarized along the z axis of the cylindrical system, we arrange the SiC rods along the r axis and form an array in the θ - z plane. The proposed structure is depicted in Fig. 4, where arrays of SiC wires along the radial direction are placed between the two surfaces of the cylindrical cloak.

The effective permeability of the system can be estimated as follows using the approach in [34]:

$$\mu_r = \frac{2}{kL_1^2} \frac{L_1 J_1(kL_1) - tJ_1(kt) + a_0 t H_1^{(1)}(kt) - a_0 L_1 H_1^{(1)}(kL_1) + c_0 t J_1(nkt)/n}{J_0(kL_2/2) - a_0 H_0^{(1)}(kL_2/2)} \quad (10)$$

where h and φ represent the periodicities along the z and θ directions respectively, t denotes the radius of each wire, $n = \sqrt{\epsilon_{\text{SiC}}}$ is the refractive index, $k = 2\pi/\lambda_0$ denotes the wave vector, $L_1 = \sqrt{hr\varphi/\pi}$ and $L_2 = (h + r\varphi)/2$ represent the two effective unit sizes based on area and perimeter estimations respectively.

$a_0 = [nJ_0(nkt)J_1(kt) - J_0(kt)J_1(nkt)]/[nJ_0(nkt)H_1^{(1)}(kt) - H_0^{(1)}(kt)J_1(nkt)]$ and $c_0 = [J_0(kt) - a_0 H_0^{(1)}(kt)]/J_0(nkt)$ are the scattering coefficients, and the Bessel functions in the equation follow the standard notations. The permittivity along the z direction is well approximated using Maxwell-Garnett method [34]. In the design we choose the appropriate transformation, geometry and operational wavelength such that the calculated effective parameters μ_r and ϵ_z follow what is required by Eq. (2) with tolerable deviations. In Fig. 5 we plot the required and the calculated μ_r and ϵ_z for a TE cloak at $\lambda = 13.5 \mu\text{m}$. The parameters used for this calculation are $a = 15 \mu\text{m}$, $a/b = 0.35$, $t = 1.2 \mu\text{m}$, $h = 2.8 \mu\text{m}$, $\varphi = 10.6^\circ$, and the p coefficient in the quadratic transformation is $0.5a/b^2$. We observe very good agreement between the required values and the calculated ones based on analytical formulae, and the imaginary part in the effective permeability is less than 0.06. This computation verifies the feasibility of the proposed cloaking system based on SiC wire arrays for the TE polarization.

5. Conclusions

In summary, using high-order transformations we proposed two novel designs of optical cloaks for TM and TE polarizations. This critical development builds upon our previous work on the design of a non-magnetic cloak and the suggestion of using high-order transformations to produce more flexible cloaking systems. We should note that the effective material properties in the two designs presented in this paper are evaluated using simple analytical models, and the bulk dielectric functions of the constituent materials are used in all

calculations. In the real-life construction of such cloaking systems, there would be expected deviations from the presented parameters in terms of particular values in the geometry and transformation functions. Nevertheless, this work provides realistic structures and models which lead to a practical path towards realizing actual cloaking devices at optical wavelengths.

Acknowledgments

The authors would like to thank our colleague Xingjie Ni for his help with 3D illustrations. This work was supported in part Army Research Office grant W911NF-04-1-0350 and by ARO-MURI award 50342-PH-MUR.